

Article

Dynamics of a prey-predator system under the influence of the Allee effect and Holling type-II functional response

K. Venkataiah, K. Ramesh

Department of Mathematics, Anurag University, Hyderabad, 500088, Telangana, India

E-mail: venkat.kambala7@gmail.com, krameshrecw@gmail.com

Received 2 October 2023; Accepted 10 December 2023; Published online 18 December 2023; Published 1 June 2024



Abstract

Capturing complicated dynamics and understanding the underlying controlling ecological processes is one of the major ecological issues. The Allee effect is an essential component in ecology, and considering it can have a substantial impact on system dynamics. In the present investigation, we analysed a prey-predator scenario in which the predator is a generalist since it feeds on prey populations and the Allee phenomenon impacts the prey population's growth. The influence of the Allee effect on the changing nature of the system is investigated. The stability and boundedness of the model's equilibria are extensively investigated. We found that including the Allee effect enhances the system's local and global behaviours through a detailed bifurcation analysis. The chaotic nature of the system is strongly impacted by the Allee effect, particularly once a specific threshold value is reached. In the study of bifurcation analysis, we looked into bifurcations such the presence of transcritical bifurcation and Hopf-bifurcation to chaos. We added stochastic perturbation to this problem by including random fluctuations in the sensitive parameters. Finally, we analysed the system's mean-square stochastic stability towards the internal equilibrium. As a result, it is discovered that the Allee effect and stochastic perturbation considerably influence the behaviour of the prey-predator system.

Keywords predator-prey model; Allee effect; transcritical bifurcation; stochastic stability.

Network Biology
ISSN 2220-8879
URL: <http://www.iaees.org/publications/journals/nb/online-version.asp>
RSS: <http://www.iaees.org/publications/journals/nb/rss.xml>
E-mail: networkbiology@iaees.org
Editor-in-Chief: WenJun Zhang
Publisher: International Academy of Ecology and Environmental Sciences

1 Introduction

Predator-prey interaction is one of the essential intersperse relationship in ecology and is thought to provide the basis for the formation the various biologic networks and the entire ecological system. The Lotka-Volterra technique is inherently unstable, even though it is commonly regarded as the most traditional predator-prey system (Kot, 2001). Therefore, the origins of the predator-prey relationship remain of interest to biomathematics (Lie et al., 2009; Kent et al., 2003; Wang et al., 2011). In an effort to make the system more realistic, an extensive amount of research has been done as of yet (Gao et al., 2013; Celik et al., 2009; Hsu et al., 2001; Brown et al., 1981). An important concept that can be applied to make population models more

realistic is the Allee phenomenon.

Allee observed in 1931 that the cluster's living condition is beneficial to population expansion, but that the density is too great, inhibiting population increase and perhaps leading to extinction owing to resource competition. According to the Allee effect, any population must have an unbiased optimum density for growth and reproduction. Predator-prey theory and Allee influence in prey development are being studied by numerous other researchers (Manna et al., 2017; Banerjee et al., 2017; Allee, 1931; Cai et al., 2015; Sen et al., 2015; Wang et al., 2011; Feng et al., 2015). It is important to recognize that Allee effects can be classified as either severe or mild before continuing. The Allee effect is associated with a population growth threshold below which it becomes negative (Dennis et al., 1989; Lai et al., 1995; Lewis et al., 1993). However, even in small populations, when the Allee effect is limited, population growth slows but remains positive (Stephens et al., 1999; Berec et al., 2007; Courchamp et al., 1999). Furthermore, the functional response, or the rate of feeding, by the predator on the prey determines the dynamic complexity of the predator-prey system. When it comes to functional responses, the most common ones among arthropod predators are Holling type II (there are also Holling types I, III, and IV). To investigate the dynamical relationship between two species predator and prey, Ivlev (1961) suggested another functional response, called Ivlev functional response: $\Omega(x) = \rho(1 - e^{-\eta x})$, where ρ, η are positive constants and represent the maximum rate of predation and the efficiency of the predator for capturing prey, respectively. It is both monotonically increasing and uniformly bounded. The predator-prey systems with Ivlev's functional response have been thoroughly studied by many renowned mathematicians and ecologists (Kamrujjaman et al., 2023; Rana et al., 2020; Das et al., 2022). Both the uniqueness and existence of limit cycles, as well as numerical calculation of phase pictures, were investigated in these empirical investigations.

The present paper is organised in the following manner: The model's (3) boundedness is discussed in Section 2. The consistency of the equiposes of the paradigm (3) was discussed in depth in Section 3. The stability of equiposes (3) was examined in Section 4 in relation to various bifurcation types, including the transcritical bifurcation and the Hopf bifurcation in the vicinity of the axial and positive equilibria for the paradigm. In Section 5, we looked at the steadiness of the stochastic system linearized paradigm (3) with mean-square fluctuations as perturbations. In Section 6, we utilise MATLAB to do numerical simulations to examine the prior theoretical conclusions.

2 Model Formulation

The advanced and widely applicable paradigm was built on the foundation of a single model of population expansion. The Lotka-Volterra paradigm has a mathematical representation.

$$\begin{aligned}\dot{x} &= r x(t) - a x(t)y(t), \\ \dot{y} &= c x(t)y(t) - m y(t).\end{aligned}\tag{1}$$

At this moment, it is well acknowledged that Allee has a significant impact on the potential of local and global extinction, and that it may generate a strong kind of dynamical impacts (Zhou et al., 2005). Examining the effects of Allee on the predator-prey paradigm is both exciting and crucial:

$$\begin{aligned}\dot{x} &= r x(t) \left(1 - \frac{x(t)}{K}\right) \frac{x(t)}{x(t) + A} - a x(t)y(t), \\ \dot{y} &= c (a x(t)) y(t) - m y(t).\end{aligned}\tag{2}$$

Here, the term $\frac{x}{x+A}$ represents weak Allee effect, where $A > 0$ indicates a constant weak Allee effect.

The amounts of prey and predator are denoted by x, y correspondingly, m is the hunters' inborn passing speed, c is the transformation proficiency from prey to hunter, K is the carrying capacity, r is the prey population's inherent increasing rate, and is the prey catch rate by their hunters. Integrating the type-II operational retort in the system (2) is exciting in order to bring the system launched in this work biologically closer to reality. Based on the foregoing, we develop the following predator-prey model with type-II operational mechanism and weak Allee effect:

$$\begin{aligned} \dot{x} &= r x(t) \left(1 - \frac{x(t)}{K} \right) \frac{x(t)}{x(t)+A} - \frac{\beta x(t) y(t)}{1 + \alpha y(t)}, \\ \dot{y} &= \frac{c(\beta x(t)) y(t)}{1 + \alpha y(t)} - m y(t). \end{aligned} \quad (3)$$

From above model (3), we can notice the three equilibrium points $E_0(0,0)$, $E_1(K,0)$ and $\tilde{E}(\tilde{x}, \tilde{y})$. Here

$$\tilde{x} = \frac{m(1 + \alpha y)}{\beta c} \quad \text{and} \quad \tilde{y} \text{ is the positive root of the cubic equation } A_0 y^3 - A_1 y^2 - A_2 y - A_3 = 0.$$

Where $A_0 = \alpha^3 r m^2$, $A_1 = \alpha^2 r m K \beta c - 3\alpha^2 m^2 r - K \beta^2 c m \alpha$, $A_2 = 2\alpha r m K \beta c - 3\alpha r m^2 - K \beta^2 c m - K A \beta^2 c^2$,

and $A_3 = r m K \beta c - r m^2$.

2.1 Boundedness

The subsequent theorem set up the boundedness of the system's solutions.

Any xy -plane solution that starts in the first quadrant will always finish in the first quadrant. As a result, as shown in Theorem 1, the solution is positive and bounded.

Theorem 1. For the model's (3) solution $(x(t), y(t))$

$$\lim_{t \rightarrow \infty} \sup \left(x(t) + \frac{1}{c} y(t) \right) \leq \frac{K(m+r)^2}{4rm}. \quad (4)$$

Proof: We consider $L = x + \frac{1}{c} y$, on the basis of the solution of the model (3), we can verify the following inequality.

$$\begin{aligned}
 \dot{L}(t) &= \dot{x}(t) + c^{-1}\dot{y}(t) \\
 &= \frac{x}{x+A} \left(rx - \frac{rx^2}{K} \right) - \frac{\beta xy}{1+\alpha y} + \frac{\beta xy}{1+\alpha y} - c^{-1}my \\
 &= \frac{x}{x+A} \left(rx - \frac{rx^2}{K} \right) - c^{-1}my \\
 \dot{L}(t) + mL &= \frac{x}{x+A} \left(rx - \frac{rx^2}{K} \right) - c^{-1}my + mx + c^{-1}my \\
 &= \frac{x}{x+A} \left(rx - \frac{rx^2}{K} \right) + mx \\
 &\leq rx \left(1 - \frac{x}{K} \right) + mx \\
 &\leq x \left(r + m - \frac{r}{K}x \right) \\
 &\leq \frac{K}{4rm} (m+r)^2.
 \end{aligned}$$

As a result, it can be said that $\lim_{t \rightarrow \infty} \sup \left(x(t) + \frac{1}{c} y(t) \right) \leq \frac{K(m+r)^2}{4rm}$. (5)

3 Stability Analysis

This section of the study emphasises on the examination of several equilibrium points and their local stability. This is achieved by analyzing the characteristic roots of the variational matrix, which is computed in the vicinity of the equilibrium points.

Let $f_1(x, y) = rx \left(1 - \frac{x}{K} \right) \frac{x}{x+A} - \frac{\beta xy}{1+\alpha y}$,

$$f_2(x, y) = \frac{c(\beta x)y}{1+\alpha y} - my. \tag{6}$$

The Jacobian matrix for model (2) can be calculated as follows: $J = \begin{pmatrix} f_{1x} & f_{1y} \\ f_{2x} & f_{2y} \end{pmatrix}$,

where $f_{1x} = \frac{-2rx^3 + (rK - 3Ar)x^2 + 2ArKx}{K(x+A)^2} - \frac{\beta y}{1+\alpha y}$, $f_{1y} = -\frac{\beta x}{(1+\alpha y)^2}$,

$$f_{2x} = \frac{c\beta y}{(1+\alpha y)}, f_{2y} = \frac{c\beta x}{(1+\alpha y)^2} - m. \tag{7}$$

The Jacobian matrix of the model (2) at $E_0(0, 0)$ is given by $J_0 = \begin{pmatrix} 0 & 0 \\ 0 & -m \end{pmatrix}$ (8)

As a result, it can be observed that E_0 is invariably a saddle node.

The variational matrix of system (2) at $E_1(K, 0)$ is given by

$$J_1 = \begin{pmatrix} \frac{-rK}{K+A} & -\beta K \\ 0 & c\beta K - m \end{pmatrix}. \quad (9)$$

Here E_1 is stable since first eigen value $\frac{-rK}{K+A}$ is negative if $c\beta K - m < 0 \Rightarrow \beta < \frac{m}{cK}$, and E_1 is saddle point when $\beta > \frac{m}{cK}$. Finally, for model (2), the Jacobian matrix may be found at \tilde{E}

$$\tilde{J} = \begin{pmatrix} \frac{-2rx^3 + rKx^2 - 3rAx^2 + 2rAKx}{K(x+A)^2} & \frac{\beta y}{1+\alpha y} & \frac{-\beta x}{(1+\alpha y)^2} \\ \frac{m}{x}y & & \frac{-c\alpha\beta xy}{(1+\alpha y)^2} \end{pmatrix}. \quad (10)$$

The latent polynomial is $C(\lambda) = \lambda^2 - Tr(\lambda) + D$, (11)

$$\text{where } Tr = \frac{-rx}{K(x+A)^2} (x^2 + 2Ax - AK) - \frac{c\alpha\beta xy}{(1+\alpha y)^2},$$

$$D = \frac{(2rx^3 - rKx^2 + 3rAx^2 - 2rAKx)c\alpha\beta xy}{K(x+A)^2(1+\alpha y)^2} + \frac{c\alpha\beta^2 xy^2}{(1+\alpha y)^3} + \frac{\beta my}{(1+\alpha y)^2}.$$

The local asymptotic stability of point \tilde{E} in scheme (3) can be easily verified by applying the Routh-Hurwitz criterion, under the condition that $A < \frac{x^2}{K-2x}$.

Theorem 2. The global resilience of equilibrium point $E_1 = (K, 0)$ is established provided the condition

$$\beta < \frac{m}{cK} \text{ holds.}$$

Proof: Let the Lyapunov function be

$$V(x, y) = \int_K^x \frac{p-K}{p} dp + \frac{1}{c} y. \quad (12)$$

Calculating V 's derivative along the model's solution

$$\begin{aligned} \dot{V}(t) &= \left(\frac{x-K}{x}\right)\dot{x}(t) + c^{-1}\dot{y}(t) \\ &= \left(\frac{x-K}{x}\right)\left[\left(rx - \frac{rx^2}{K}\right)\frac{x}{x+A} - \frac{\beta xy}{1+\alpha y}\right] + \frac{\beta xy}{1+\alpha y} - c^{-1}my \\ &= \frac{x}{x+A}\left[r(x-K)\left(1 - \frac{x}{K}\right)\right] - \frac{\beta y}{1+\alpha y}(x-K) + \frac{\beta xy}{1+\alpha y} - c^{-1}my \\ &= (x-K)\left[\frac{rKx - rx^2}{K(x+A)}\right] + \frac{\beta yK}{1+\alpha y} - c^{-1}my \\ &\leq \frac{\beta Ky}{1+\alpha y} - c^{-1}my \end{aligned}$$

4 Bifurcation Analysis

This section focuses on how equilibrium points appear and vanish, as well as how the stability of equilibria changes as a result of various types of bifurcations.

4.1 Transcritical bifurcation

Theorem 3. When $\beta = \beta_0$, with $\beta = \frac{m}{cK}$, the model undergoes transcritical bifurcation in the region around

E_1 .

Proof: If $J_1 = 0$, one of the characteristic roots will be zero which gives $\beta = \beta_0$. $\frac{-rK}{K+A}$ is currently another characteristic root. Let V and W be the characteristic vectors with respect to the characteristic root zero of the matrices J_1 and J_1^T , we get

$$J_1 = \begin{pmatrix} \frac{-rK}{K+A} & -\beta K \\ 0 & 0 \end{pmatrix}, V = \begin{pmatrix} -\beta(K+A) \\ r \\ 1 \end{pmatrix} \text{ and } J_1^T = \begin{pmatrix} \frac{-rK}{K+A} & 0 \\ -\beta K & 0 \end{pmatrix}, W = \begin{pmatrix} 0 \\ 1 \end{pmatrix}.$$

$$W^T f_\beta(\bar{x}, \bar{y}, \beta_0) = 0,$$

$$W^T \left[Df_\beta(\bar{x}, \bar{y}, \beta_0) V \right] = cK \neq 0,$$

$$\begin{aligned} W^T \left[D^2 f(\bar{x}, \bar{y}, \beta_0)(VV) \right] &= W^T \begin{pmatrix} \frac{\partial^2 f_1}{\partial x^2} V_1^2 + 2 \frac{\partial^2 f_1}{\partial x \partial y} V_1 V_2 + \frac{\partial^2 f_1}{\partial y^2} V_2^2 \\ \frac{\partial^2 f_2}{\partial x^2} V_1^2 + 2 \frac{\partial^2 f_2}{\partial x \partial y} V_1 V_2 + \frac{\partial^2 f_2}{\partial y^2} V_2^2 \end{pmatrix}_{(\bar{x}, \bar{y}, \beta_0)}, \\ &= \frac{-2c\beta^2(K+A)}{r} - 2c\alpha\beta K \neq 0. \end{aligned} \tag{13}$$

Therefore, the system has transcritical bifurcation at $\beta = \beta_0$ around the axial equilibrium E_1 (Sotomayor

theorem, Perko, 2001).

4.2 Hopf bifurcation

The system undergoes bifurcation if $A = \frac{x^2}{K - 2x}$. Next, we have to show that system (2) experiences a Hopf

bifurcation if $A = \frac{x^2}{K - 2x}$. By choosing a suitable parameter, we investigate the Hopf bifurcation at

$$E_* = (x_*, y_*).$$

$$\text{Let } A_0 = \frac{x_*^2}{K - 2x_*}. \quad (14)$$

If $A = A_0$, then $T = 0$ and the Jacobian matrix \tilde{J} will have the couple of imaginary characteristic roots

$\lambda = \pm i\sqrt{m\alpha\tilde{y}}$. Let $\lambda = L(A) \pm iM(A)$ be the roots of $\lambda^2 - T\lambda + D = 0$, then

$$\begin{aligned} L^2 - M^2 - LT + D &= 0, \\ 2LM - TM &= 0, \end{aligned} \quad (15)$$

$$\text{and } L = \frac{T}{2}, M = \frac{1}{2}\sqrt{4D - T^2}. \quad (16)$$

$$\begin{aligned} \frac{dL}{dA} &= \frac{d}{dA} \left\{ \frac{-rx}{K(x+A)^2} (x^2 + 2Ax - AK) - \frac{c\alpha\beta xy}{(1+\alpha y)^2} \right\} \\ &= \frac{-rx}{K(x+A)^3} \{AK - x(K+2A)\} \end{aligned}$$

$$\left. \frac{dL}{dA} \right|_{A=A_0} = \frac{-rx}{K(x+A)^3} [AK - x(K+2A)] < 0.$$

If $AK > x(K+2A) \Rightarrow A > \frac{Kx}{K-2x}$, on using the result of Poincare-Andronov-Hopf bifurcation theorem, we

say that the system (2) at \tilde{E} go through a Hopf bifurcation. As a result, system (2) admits a Hopf bifurcation at $A = A_0$ corresponding to \tilde{E} .

5 Stochastic Analysis

In this section, we used the white noise approach to characterize the external disruptions on the system (3). We explain all of this at the coexistence equilibrium point. We investigate the linearized model with perturbations to account for the stability of the stochastic system. We compute the population intensities of noise-induced fluctuations (variances) around the positive equilibrium using the methodology developed by Nisbet and Gurney (1982) and Carletti (2006). The perturbed stochastic model can be expressed as

$$\frac{dx(t)}{dt} = \left[rx \left(1 - \frac{x}{K} \right) \frac{x}{x+A} - \frac{\beta xy}{1+\alpha y} \right] dt + p_1 \xi_1(t), \tag{17}$$

$$\frac{dy(t)}{dt} = \left[\frac{c(\beta x)y}{1+\alpha y} - my \right] dt + p_2 \xi_2(t).$$

The aforementioned system is linearized by incorporating the perturbations $x_1(t)$ and $x_2(t)$

i.e., $S = x_1 + S^*, I = x_2 + I^*$ then

$$\frac{dx_1(t)}{dt} = -\frac{1}{A} 2rx_1x^* - \beta y_1x^* + p_1 \xi_1(t), \tag{18}$$

$$\frac{dx_2(t)}{dt} = c\beta x_1y^* + p_2 \xi_2(t).$$

Both sides are subjected to Fourier transformations, and the result is

$$p_1 \xi_1(t) = i\omega \tilde{x}_1(\omega) + \beta x^* \tilde{y}_1(\omega) - \frac{1}{A} 2rx^* \tilde{x}_1(\omega),$$

$$p_2 \xi_2(t) = i\omega \tilde{y}_1(\omega) - c\beta y^* \tilde{x}_1(\omega).$$

The aforementioned system can be expressed in matrix form as

$$\bar{\xi}(\omega) = Q(\omega) X(\omega), \tag{19}$$

where the elements of $Q(\omega)$ are $q_{11}, q_{12}, q_{21}, q_{22}$ (row wise) then $Q(\omega) = \begin{bmatrix} q_{11} & q_{12} \\ q_{21} & q_{22} \end{bmatrix}$ and

$$\bar{\xi}(\omega) = \begin{bmatrix} p_1 \xi_1(t) \\ p_2 \xi_2(t) \end{bmatrix}, X(\omega) = \begin{bmatrix} x_1(\omega) \\ x_2(\omega) \end{bmatrix}, q_{11} = i\omega - \frac{1}{A} 2rx^*, q_{12} = \beta x^*, q_{21} = -c\beta y^*, q_{22} = i\omega,$$

$Q(\omega)$ has an inverse, and knowing that it is a non-singular matrix, hence from (19) we get

$$X(\omega) = Q^{-1}(\omega) \bar{\xi}(\omega) = P(\omega) \bar{\xi}(\omega). \tag{20}$$

Where $P(\omega) = \frac{AdjQ(\omega)}{|Q(\omega)|} = \begin{bmatrix} p_{11} & p_{12} \\ p_{21} & p_{22} \end{bmatrix}$

The spectral density is employed to establish the following definition

$$S_g(\omega) d\omega = \lim_{T \rightarrow \infty} \frac{\overline{|g(\omega)|^2}}{T}.$$

Assuming that $g(t)$ a random function with a mean of zero and that $S_g(\omega)$ is the variance of $g(t)$'s elements of inside the interval $[\omega, \omega + d\omega]$.

An auto covariance function is provided by the inverse transform of $S_g(\omega)$

$$C_g(\tau') = \frac{1}{2\pi} \int_{-\infty}^{\infty} S_g(\omega) e^{i\omega\tau'} d\omega,$$

and $g(t)$'s variance function is expressed as

$$\sigma_g^2 = C_g(0) = \frac{1}{2\pi} \int_{-\infty}^{\infty} S_g d\omega.$$

From (14), the mean value of the population is $\bar{x}_i = \sum_{j=1}^2 p_{ij} \xi_j(\omega)$ where $b_{ij}, i, j = 1, 2$.

Therefore, $S_{x_i} = \sum_{j=1}^2 q_j |p_{ij}(\omega)|^2$, ($i = 1, 2$).

The fluctuations of $x_i (i = 1, 2)$ are expressed as

$$\sigma_{x_i}^2 = \frac{1}{2\pi} \int_{-\infty}^{\infty} S_{x_i} d\omega = \frac{1}{2\pi} \sum_{j=1}^2 \int_{-\infty}^{\infty} q_j |p_{ij}(\omega)|^2 d\omega.$$

By using system (11) with the aforementioned variances, we can thus find

$$\begin{aligned} \sigma_{x_1}^2 &= \frac{1}{2\pi} \left[q_1 \int_{-\infty}^{\infty} \left| \frac{A_1}{Q(\omega)} \right|^2 d\omega + q_2 \int_{-\infty}^{\infty} \left| \frac{B_1}{Q(\omega)} \right|^2 d\omega \right], \\ \sigma_{x_2}^2 &= \frac{1}{2\pi} \left[q_1 \int_{-\infty}^{\infty} \left| \frac{A_2}{Q(\omega)} \right|^2 d\omega + q_2 \int_{-\infty}^{\infty} \left| \frac{B_2}{Q(\omega)} \right|^2 d\omega \right], \end{aligned} \quad (21)$$

where $|Q(\omega)| = Q_1(\omega) + iQ_2(\omega)$ and $Q_1(\omega) = -\omega^2 + c\beta^2 x^* y^*$, $Q_2(\omega) = -\frac{1}{A} 2rx^* \omega$

where $|A_1|^2 = \omega^2$, $|B_1|^2 = (\beta x^*)^2$, $|A_2|^2 = (c\beta y^*)^2$, $|B_2|^2 = \omega^2 + \left(\frac{1}{A} 2rx^*\right)^2$.

The variances of the system (17) populations x and y are given in (21). The majority of the time, finding these integrals is difficult. We can easily explain these outcomes using mathematical re-enactments in this way. Taking different boundary values and calculating the difference over time, if the difference is small, the related population is stable, but unstable.

6 Numerical Simulations

In this portion, we use MATLAB software to provide numerical simulations to validate our mathematical conclusions and to explore the impact of the Allee parameter with Holling type - II operating retort and stochasticity on the dynamics of the two species.

Example 1.

We illustrate the behaviour of system (3) across the concomitance equipoise by taking the parameter values $r = 0.2640, K = 69.2, A = 0.1, \beta = 0.938, \alpha = 0.646, c = 0.882, m = 0.345$, we observe that system (3) converges

globally towards the coexisting equilibrium (see Fig. 1). If we increase the value of $A = 0.126$ and keep the other parameters fixed, from Fig. 2 and Fig. 3, the positive equilibrium appears to be losing its stability. The Hopf-bifurcation of system (3) near positive equilibrium at $A = A_0$ is shown in Fig. 3.

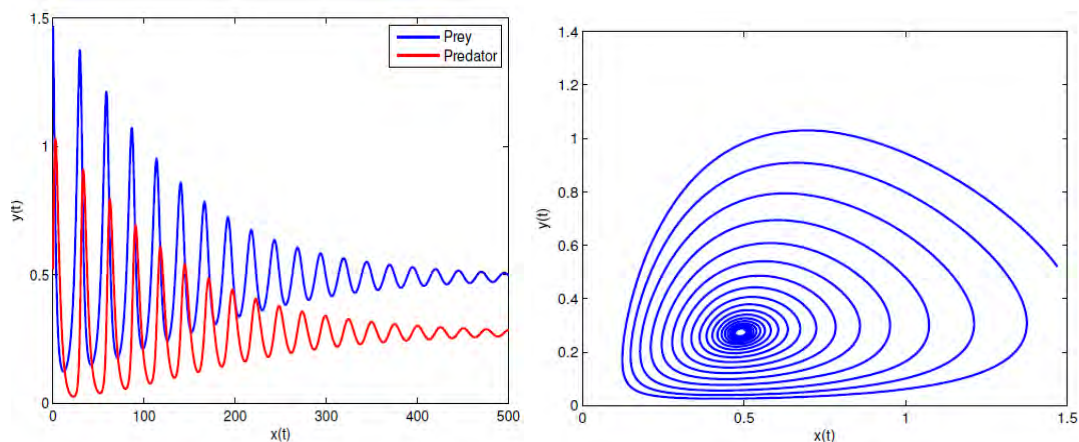


Fig. 1 The stability of the concomitant equipose of system (3).

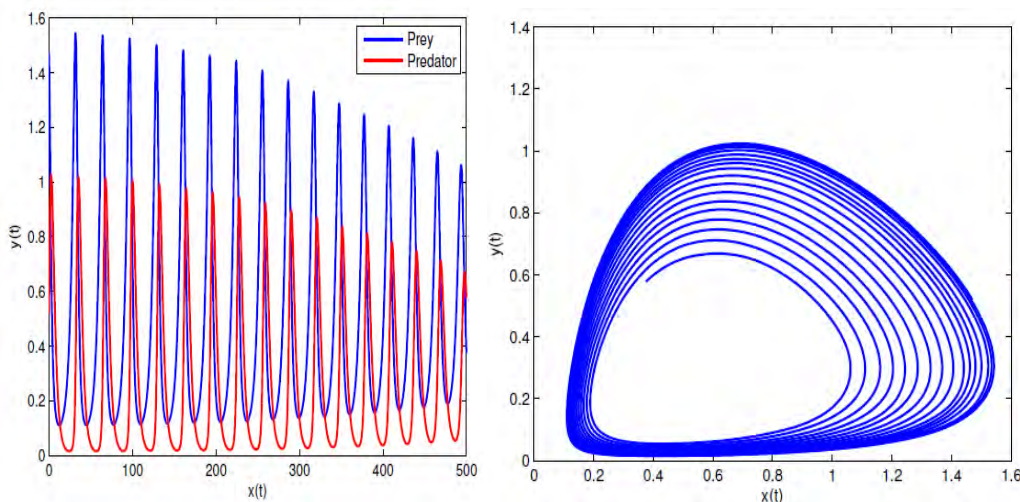


Fig. 2 Local asymptotic stability of the concomitant equipose of system (3) corresponding to $A = 0.126$.

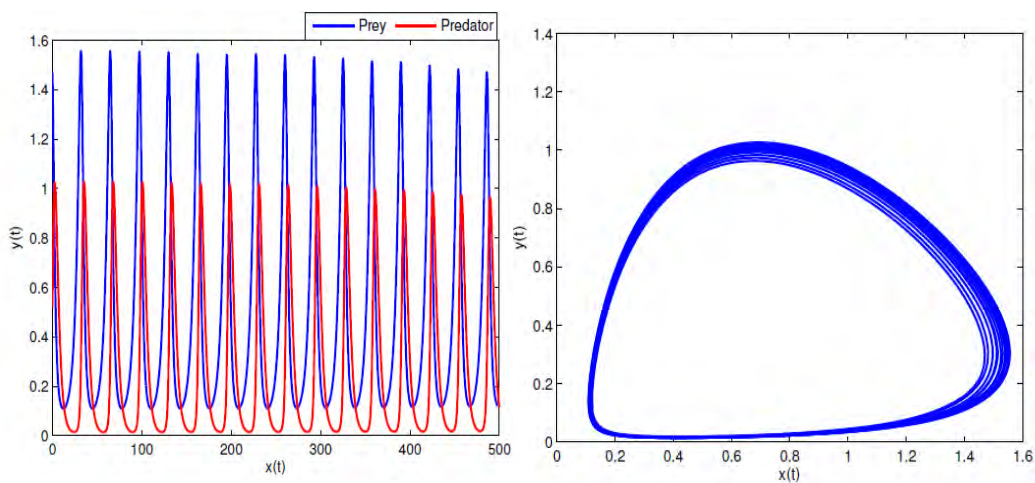


Fig. 3 Local asymptotic stability of the concomitant equipose of system (3) corresponding to $A = 0.128$.

Example 2. Taking the parameter values as $r = 0.2640, K = 11, A = 0.128, \beta = 0.76, \alpha = 0.646, c = 0.882, m = 0.345$, and white noises $\sigma_1 = 0.05, \sigma_2 = 0.01$.

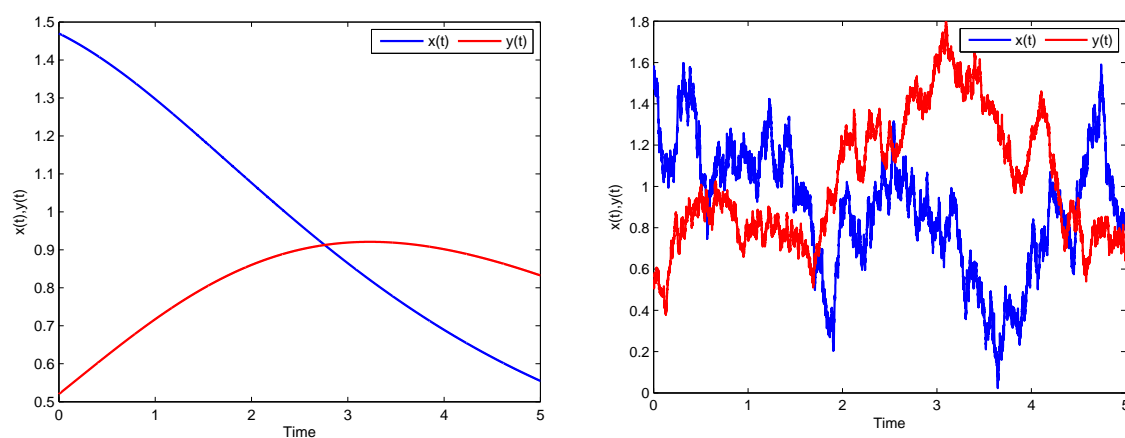


Fig. 4 Trajectories of the deterministic system (3) (left figure) and the stochastic system (17).

Fig. 4 depicts the system's deterministic and stochastic courses (3). We learned that when the noise is strong enough, it can confine the population, causing it to fluctuate to a substantial amount. In these instances, the stochastic model may be employed to explore the population's dynamics.

7 Conclusions

In this work, we develop the traditional predator-prey scheme, which has a weak Allee effect. We then demonstrate and examine the stability and boundedness of the model. We also showed that for $A = A_0$, the model (3) features a transcritical bifurcation near the axial equilibrium and a Hopf bifurcation at $\tilde{E} = (\tilde{x}, \tilde{y})$. To meet the stable criteria, we pick the necessary parameters initially. Then we attempt to fluctuate the value of constraint A later, including the timing, phase, and bifurcation diagrams for individually constraint depicted. As A rises, the model (3) will induce bifurcation, which adds to our conclusion. From a biological standpoint, it is worth noting that there are some differences which will alter the model's stability by inclusion of a weak Allee effect, i.e., the model's stable state across populations will be disrupted. In addition, we explored the system's stochastic stability by integrating white noise perturbations. White noise has an effect on the system's stability, according to our research (Fig. 4).

Acknowledgment

The authors are very grateful to the reviewers for their time, valuable comments and helpful suggestions which have significantly improved the quality of the manuscript. Also, the support from Department of Mathematics, Anurag University is greatly acknowledged. Both authors contributed equally and significantly in writing this paper and typed, read, and approved the final manuscript.

References

- Allee WC. 1931. *Animal Aggregations: A Study in General Sociology*. University of Chicago Press, Chicago, USA
- Banerjee M, Takeuchi. Y. 2017. Maturation delay for the predators can enhance stable coexistence for a class of prey-predator models. *Journal of Theoretical Biology*, 412: 154 -171
- Berec L, Angulo, E, Courchamp. F. 2007. Multiple Allee effects and population management. *Trends in Ecology Evolution*, 22: 185-191
- Brown KJ, Dume PC, Gardner RA. 1981. A similinear parabolic system arising in the theory of superconductivity. *Journal of Differential Equations*, 40(2): 232-252
- Cai Y, Zhao C, Wang W, Wang J. 2015. Dynamics of a Leslie–Gower predator-prey model with additive Allee effect. *Applied Mathematical Modelling*, 39(7): 2092–2106
- Carletti M. 2006. Numerical solution of stochastic differential problems in the biosciences. *Journal of Computational and Applied Mathematics*, 185(2): 422-440
- Celik C, Duman O. 2009. Allee effect in a discrete-time predator-prey system. *Chaos, Solitons and Fractals*, 40(4): 1956-1962.
- Courchamp F, Clutton-Brock T, Grenfell B. 1999. Inverse density dependence and the Allee effect. *Trends in Ecology Evolution*, 14: 405-410
- Das K, Kumar R, Das P. 2022. Impact of periodicity and stochastic impact on COVID-19 pandemic: A mathematical model. *Network Biology*, 12(3): 120-132
- Dennis B. 1989. Allee effects: Population growth, critical density, and the chance of extinction. *Natural Resource Modelling*, 3: 481-538
- Feng P, Kang Y. 2015. Dynamics of a modified Leslie–Gower model with double Allee effects. *Nonlinear Dynamics*, 80(1-2): 1051-1062
- Hsu SB, Hwang TW, Kuang Y. 2001. Global analysis of the Michaelis-Menten type ratio-dependent predator-prey system, *Journal of Mathematical Biology*, 42(6): 489–506
- Ivlev VS. 1961. *Experimental Ecology of the Feeding of Fishes*. Yale University Press, Kentucky, USA
- Kamrujjaman MD, Akter SI, Akhi AA, et al. 2023. Monte Carlo sampling and computational analysis of a three component tumor radiotherapy mathematical model. *Network Biology*, 13(4): 213-229
- Kent A, Patric Doncaster C, Sluckin T. 2003. Conquences for predators of rescue and Allee effects on prey. *Ecological Modelling*, 162(3): 233-245
- Kot M. 2001. *Elements of Mathematical Ecology*. Cambridge University Press, Cambridge, UK
- Lai YC, Winslow RL. 1995. Geometric properties of the chaotic saddle responsible for super transients in spatiotemporal chaotic systems. *Physical Review Letters*, 74: 5208
- Lewis MA, Kareiva P. 1993. Allee dynamics and the spread of invading organisms. *Theoretical Population Biology*, 43: 141-158
- Liu H, Li Z, Gao M. 2009. Dynamics of a host-parasitoid model with Allee effect for the host and parasitoid aggregation. *Ecological Complexity*, 6(3): 337-345
- Manna D, Maiti A, Samanta GP. 2017. A Michaelis–Menten type food chain model with strong Allee effect on the prey. *Applied Mathematics and Computation*, 311: 390-409
- Nisbet RM, Gurney WSC. 1982. *Modelling Fluctuating Populations*, John Wiley, New York, USA
- Perko L. 2001. *Differential Equations and Dynamical Systems*. Springer, New York, USA

- Rana SM. 2020. Chaotic dynamics and control in a discrete-time predator-prey system with Ivlev functional response. *Network Biology*, 10(2): 45-61
- Sen M, Banerjee M. 2015. Rich global dynamics in a prey-predator model with Allee effect and density dependent death rate of predator. *International Journal of Bifurcation and Chaos*, 25(03): 1530007
- Stephens PA, Sutherland WJ. 1999. Consequences of the Allee effect for behaviour, ecology and conservation. *Trends in Ecology Evolution*, 14: 401-405
- Wang J, Shi J, Wei J. 2010. Predator-prey system with strong Allee effect in prey. *Journal of Mathematical Biology*, 62(3): 291-331
- Wang WX, Zhang YB, Liu CZ. 2011. Analysis of a discrete time predator prey system with Allee effects. *Ecological Complexity*, 8(1): 81-85
- Yujing G, Bingtuan Li. 2013. Dynamics of a ratio dependent predator-prey system with a strong Allee effect. *Discrete and Continuous Dynamical Systems-B*, 18(9): 2283-2313
- Zhou SR, Liu YF, Wang G. 2005. The stability of predator-prey systems subject to the Allee effects. *Theoretical Population Biology*, 67(1): 23-31